



PERGAMON

Available online at www.sciencedirect.com

SCIENCE @ DIRECT®

Solid-State Electronics xxx (2003) xxx–xxx

SOLID-STATE
ELECTRONICSwww.elsevier.com/locate/sse

Ferromagnetism in Mn- and Cr-Implanted AlGaP

M.E. Overberg^{a,*}, G.T. Thaler^a, R.M. Frazier^a, R. Rairigh^b, J. Kelly^b,
C.R. Abernathy^a, S.J. Pearton^a, A.F. Hebard^b, R.G. Wilson^c, J.M. Zavada^d

^a Department of Materials Science and Engineering, University of Florida, Gainesville, FL 32611, USA

^b Department of Physics, University of Florida, Gainesville, FL 32611, USA

^c Consultant, Stevenson Ranch, CA 91381, USA

^d US Army Research Office, Research Triangle Park, NC 27709, USA

Received 17 November 2002; received in revised form 21 January 2003; accepted 5 March 2003

Abstract

Implantation of Mn or Cr at doses of $3\text{--}5 \times 10^{16} \text{ cm}^{-2}$ into Si-doped $\text{Al}_{0.24}\text{Ga}_{0.76}\text{P}$ epilayers on GaP substrates produced ferromagnetic ordering at temperatures up to 300 K. The results were similar to those obtained previously in p-type AlGaP(C), indicating that both electron and hole-doped AlGaP can exhibit ferromagnetism. In addition, the AlGaP results are similar to those for GaP so the magnitude of the bandgap was not the main parameter influencing the Curie temperature, in contradiction to predictions from some mean-field theories. Second phases were not observed by X-ray diffraction and were not responsible for the ferromagnetism.

© 2003 Published by Elsevier Science Ltd.

1. Introduction

Wide bandgap semiconductors such as GaN, AlN and ZnO have recently been shown to exhibit room temperature ferromagnetism when doped with transition metals such as Mn and Cr [1–15]. This raises the possibility of spintronic devices such as transistors which exploit the spin of the electron or light-emitters with polarized output. The more common semiconductors such as GaAs have Curie temperatures well below room temperature and are therefore less attractive for device applications. In this regard, GaP shows promise because it is almost lattice-matched to Si and it would be possible to integrate GaP-based spintronic devices with existing Si microcircuitry. Recent reports have shown room temperature ferromagnetism in GaP implanted with Mn or doped with this element during growth by molecular beam epitaxy [1,2]. A potential device structure using GaMnP integrated into a Si/SiGe field effect transistor is shown in Fig. 1. In this so-called Datta-Das [16] configuration the GaMnP is used as the spin current injector

and collector, while the transistors channel is comprised of SiGe.

Another promising material for room temperature spintronic devices is AlGaP doped with transition elements. The bandgap is larger than for pure GaP and AlGaP is already used in devices such as light-emitting diodes, heterostructure field effect transistors and heterojunction bipolar transistors. In this paper we report on the magnetic properties of Mn^+ and Cr^+ implanted $\text{Al}_{0.24}\text{Ga}_{0.76}\text{P}(\text{Si})$. The results are similar to those obtained for AlGaP(C), showing that both electrons and holes are capable of inducing ferromagnetism in this material.

2. Experimental

$\text{Al}_{0.24}\text{Ga}_{0.76}\text{P}:\text{Si}$ layers were grown on undoped GaP substrates using gas source molecular beam epitaxy. The Al was provided by a dimethylethylamine alane (DMEAA) bubbler source using ultrapure He as a carrier gas. The Ga was provided by a shuttered effusion oven held at 955 °C charged with 7 N (99.99999% pure) material. The Si for electrical doping was provided by SiBr_4 pyrolyzed at the substrate surface. Thermally

* Corresponding author.

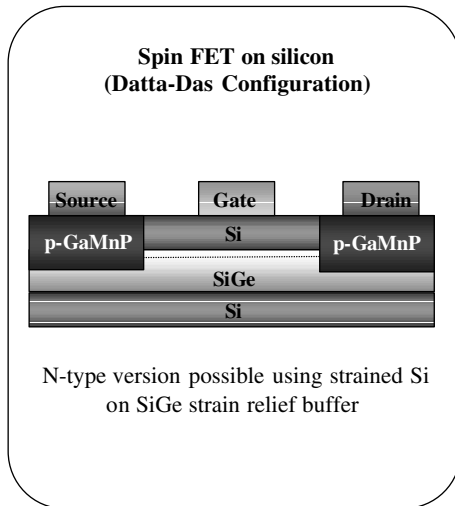


Fig. 1. Potential GaMnP/Si/SiGe spinfet.

cracked PH_3 provided the group V species, the cracker being held at a temperature of 1050°C . A growth temperature of 650°C was used for the films, whose thickness was typically $0.5\ \mu\text{m}$. The n-type doping concentration was $\sim 5 \times 10^{18}\ \text{cm}^{-3}$ for the epilayers, as measured by the Hall effect. Implants of $250\ \text{keV}\ \text{Mn}^+$ or Cr^+ ions were performed at 350°C at doses from 3 to $5 \times 10^{16}\ \text{cm}^{-2}$. These doses correspond to peak volume concentrations of 3 – $5\ \text{at.}\%$ at a distance of $\sim 1500\ \text{\AA}$ from the surface. Following implantation, the samples were annealed at 700°C for $5\ \text{m}$ under flowing N_2 to remove lattice disorder. Structural analysis was performed in situ via reflection high energy electron diffraction (RHEED), and ex situ via high-resolution X-ray diffraction (HRXRD) in a Philips MPD X'pert diffractometer. Transmission electron microscopy (TEM) was performed in a JOEL 200CX. Magnetic measurements were performed in a quantum design superconducting quantum interference device (SQUID) magnetic properties measurement system.

3. Results and Discussion

Fig. 2 (top) shows magnetization versus applied field at $100\ \text{K}$ (M vs. H) for AlGaP implanted with $3 \times 10^{16}\ \text{cm}^{-2}$ Cr. Contributions from diamagnetism have been subtracted out of the data. The coercive field is $\sim 270\ \text{Oe}$ at $100\ \text{K}$ and $\sim 220\ \text{Oe}$ at $10\ \text{K}$. The calculated moment, $M_0 = g\mu_B S$ at $100\ \text{K}$ is ~ 0.68 Bohr magnetons (μ_B) per Mn ion and is less than the theoretical value expected for Cr ($4\ \mu_B$) if all of the Cr were participating in the ferromagnetic signal. The bottom of Fig. 2 shows the field-cooled (FC) and zero-field-cooled (ZFC) magnetization as a function of temperature for an applied

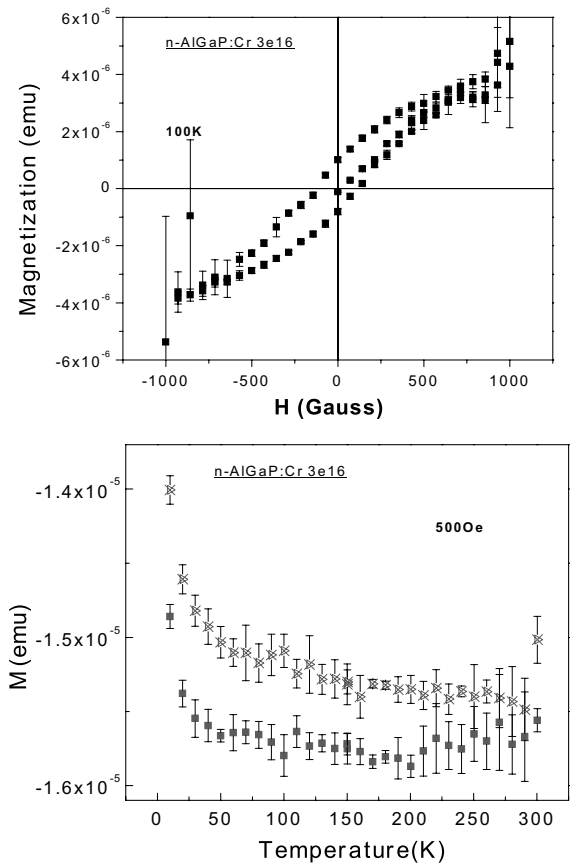


Fig. 2. (top) Magnetization at $100\ \text{K}$ versus applied field for AlGaP implanted with Cr ($3 \times 10^{16}\ \text{cm}^{-2}$) and (bottom) field-cooled and zero-field-cooled magnetization as a function of temperature at a field of $500\ \text{Oe}$.

field of $500\ \text{Oe}$. The subtraction of FC and ZFC magnetization eliminated paramagnetic contributions and indicates the presence of hysteresis if the difference is non-zero. [1] The difference in these signals persists even at $300\ \text{K}$. This is a similar result to that obtained for p-type AlGaP implanted and annealed under the same conditions. [17]

Fig. 3 shows similar data for AlGaP implanted with a higher dose of Cr, namely $5 \times 10^{16}\ \text{cm}^{-2}$. There is still a strong hysteresis loop at $100\ \text{K}$ but the overall magnetization is lower than for the $3 \times 10^{16}\ \text{cm}^{-2}$ dose. This is consistent with past results in other semiconductor systems and is evidence that second phases are not responsible for the observed properties [1], since the magnetization would be expected to increase with higher Cr^+ doses if phases such as CrO_2 were the cause of the ferromagnetism. Other potential second phases such as Cr or Al_xCr_y are not ferromagnetic in the temperature range investigated here. XRD scans revealed only the epi and substrate peaks.

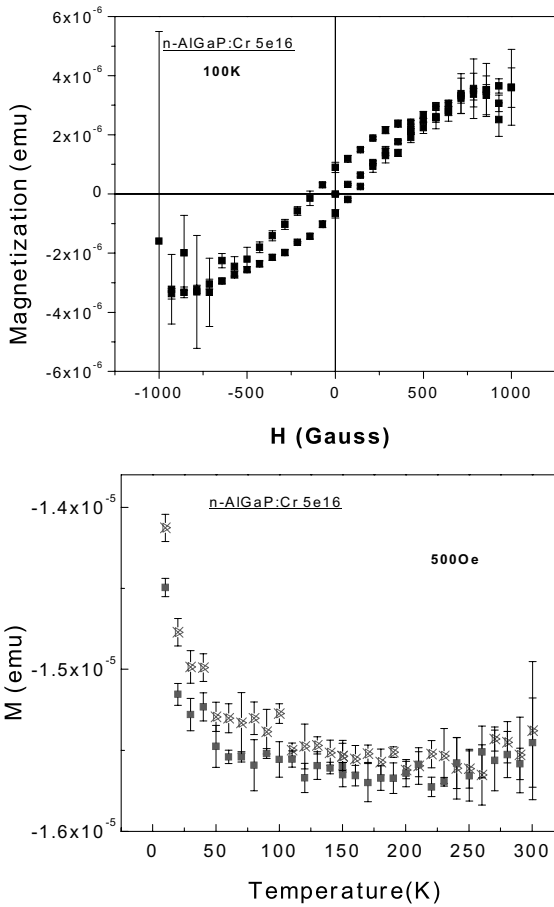


Fig. 3. (top) Magnetization at 100 K versus applied field for AlGaP implanted with Cr ($5 \times 10^{16} \text{ cm}^{-2}$) and (bottom) field-cooled and zero-field-cooled magnetization as a function of temperature at a field of 500 Oe.

The difference in FC and ZFC magnetization for the Cr-implanted AlGaP ($3 \times 10^{16} \text{ cm}^{-2}$ dose) is shown in Fig. 4. The apparent T_C is $\leq 250 \text{ K}$, which again is similar to the results obtained in p-type AlGaP(C) doped with Cr

Fig. 5 shows M vs. H data for Mn-implanted AlGaP at both 100 K (top) and 300 K (bottom). The overall magnetization is weaker than for Cr, with a calculated saturation moment of $\sim 0.22 \mu_B$ per Mn, compared to the theoretical value of 5. The low saturation moments again suggest only a small fraction of the implanted Mn ions are contributing to the observed ferromagnetism. Residual lattice disorder from the implant process and/or randomly positioned (non-substitutional) Mn ions may produce a wide distribution of exchange couplings that would weaken the ferromagnetism.

Thus, both electron- and hole-doped AlGaMnP shows ferromagnetic ordering and this is implanted from the viewpoint of p–n junction spin devices such as light-

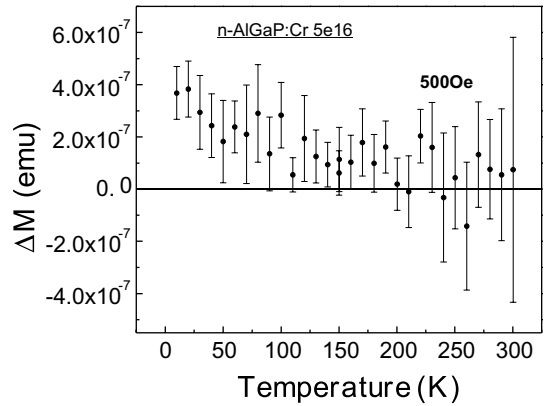


Fig. 4. Difference in field-cooled and zero-field-cooled magnetization as a function of temperature for AlGaP implanted with Cr ($5 \times 10^{16} \text{ cm}^{-2}$).

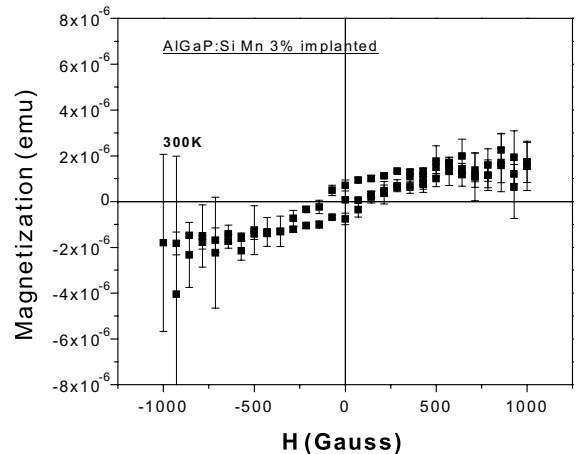
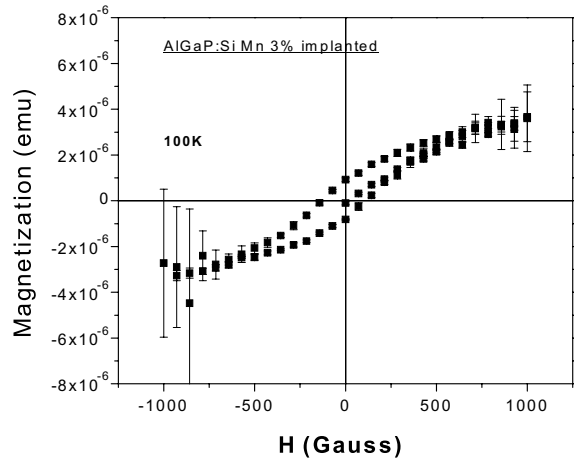


Fig. 5. (top) Magnetization at 100 K (top) or 300 K (bottom) versus applied field for AlGaP implanted with Mn ($3 \times 10^{16} \text{ cm}^{-2}$).

emitting diodes where both sides of the junction could be used for spin current injection. The origin of the observed ferromagnetism is not clear and may involve carrier-mediation mechanism inherent in the mean-field models. Another possible mechanism for the observed magnetic properties is that the Mn and Cr are not randomly distributed on group III sites but are present as atomic scale clusters. Some mean field theories suggest that Mn clustering can significantly influence T_C as a result of the localization of spin polarized holes near regions of higher Mn concentration [10]. There is also some support for this assertion from local spin density approximation calculations which predict it is energetically favorable for the formation of magnetic ion dimers and trimers at second nearest-neighbor sites which are ferromagnetic [10]. The percolation network-like model for ferromagnetism in low carrier concentration systems suggested by several groups is another potential mechanism [3].

4. Summary and conclusions

The magnetic properties of n-type AlGaP films implanted with Cr or Mn are similar to those of p-type AlGaP doped in the same fashion. No improvement in Curie temperature for transition metal doped AlGaP over GaP was observed, in contradiction to the predictions of some mean-field theories [18–20]. The magnetization was larger for Cr-doping relative to Mn-doping and second phases were not detected in the samples. Spin-based devices such as transistors lattice-matched to Si may be possible using AlGaP as the injection material.

Acknowledgements

The work at UF was partially supported by NSC MDR0101438 and ECD 02242203 and by ARO under DAAD 190110701 and 19021420.

References

- [1] Theodoropoulou N, Hebard AF, Overberg ME, Abernathy CR, Pearton SJ, Chu SNG, et al. *Phys Rev Lett* 2002;89:107203.
- [2] Overberg ME, Gila BP, Thaler GT, Abernathy CR, Pearton SJ, Theodoropoulou N, et al. *J Vac Sci Technol B* 2002;20:969.
- [3] Bhatt RN, Berciu M, Kennett MD, Wan X. *J Superconductivity: Incorporating Novel Magnetism* 2002;15:71.
- [4] Theodoropoulou N, Lee KP, Overberg ME, Chu SNG, Hebard AF, Abernathy CR, et al. *J Nanosci Nanotech* 2001;1:1012.
- [5] Theodoropoulou N, Hebard AF, Overberg ME, Abernathy CR, Pearton SJ, Chu SNG, et al. *Appl Phys Lett* 2001;78:3475.
- [6] Theodoropoulou N, Hebard AF, Overberg ME, Pearton SJ, Abernathy CR, Chu SNG, et al. *J Appl Phys* 2002; 91:7499.
- [7] Theodoropoulou N, Overberg MR, Chu SNG, Hebard AF, Abernathy CR, Wilson RG, et al. *Phys Stat Sol B* 2001;228:337.
- [8] Theodoropoulou N, Hebard AF, Chu SNG, Overberg ME, Abernathy CR, Pearton SJ, et al. *Appl Phys Lett* 2001;79:3452.
- [9] Pearton SJ, Abernathy CR, Norton DP, Hebard AF, Park YD, Boatner LA, et al. *Mater Sci Eng R* 2003;40:137.
- [10] van Schilfgarde M, Mryasov ON. *Phys Rev B* 2001; 63:233205.
- [11] Park SE, Lee H-J, Cho YC, Jeong S-Y, Cho CR, Cho S. *Appl Phys Lett* 2002;80:4187.
- [12] Yang SG, Pakhomov AB, Hung ST, Wong CY. *Appl Phys Lett* 2002;81:2418.
- [13] Hashimoto M, Zhou YK, Kanamura M, Asaki H. *Solid State Commun* 2002;122:37.
- [14] Pearton SJ, Abernathy CR, Overberg ME, Thaler GT, Norton DP, Theodoropoulou N, et al. *J Appl Phys* 2003;93:1.
- [15] Hashimoto M, Zhou Y, Kanamura M, Asaki H. *Solid State Commun* 2002;122:37.
- [16] Datta S, Das B. *Appl Phys Lett* 1990;56:665.
- [17] Overberg ME et al., *J Appl Phys*, in press.
- [18] Dietl T, Ohno H, Matsukura F, Cibert J, Ferrand D. *Science* 2000;287:1019.
- [19] Dietl T, Ohno H, Matsukura F. *Phys Rev B* 2001; 63:195205.
- [20] Dietl T. *J Appl Phys* 2001;89:7437.